International Journal of Applied Earth Observation and Geoinformation 123 (2023) 103479

Contents lists available at ScienceDirect

International Journal of Applied Earth Observation and Geoinformation

journal homepage: www.elsevier.com/locate/jag

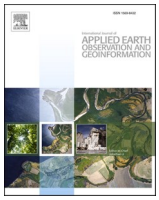

GEOV2: Improved smoothed and gap filled time series of LAI, FAPAR and FCover 1 km Copernicus Global Land products

Aleixandre Verger [a,b,*], Jorge Sánchez-Zapero [c], Marie Weiss [d], Adrià Descals [b], Fernando Camacho [c], Roselyne Lacaze [e], Frédéric Baret [d]

[a] CIDE, CSIC-UV-GVA, 46113 València, Spain
[b] CREAF, 08193 Cerdanyola del Vallès, Catalonia, Spain
[c] EOLAB, 46980 Paterna, València, Spain
[d] INRAE, Avignon Université, UMR1114 EMMAH, 84914 Avignon, France
[e] HYGEOS, 59000 Lille, France

ARTICLE INFO

Keywords:
Global vegetation monitoring
Leaf area index
Fraction of absorbed PAR
Green vegetation cover
SPOT/VGT
PROBA-V

ABSTRACT

Essential vegetation variables including leaf area index (LAI), fraction of absorbed photosynthetic active radiation (FAPAR) and fraction of green vegetation cover (FCover) are produced and distributed in the Copernicus Global Land Service. We describe here the algorithmic principles, consistency and improvements of GEOV2, Version 2 of LAI, FAPAR and FCover products derived from SPOT/VGT (1999–2013) and PROBA-V data (2014–2020) at 1 km resolution, as compared to the earlier version GEOV1. GEOV2 is based on neural networks first trained with CYCLOPES and MODIS products to estimate LAI, FAPAR and FCover from daily top of canopy reflectance. Temporal techniques are then applied to filter, smooth, fill gaps and get a composited value every 10 days. Results show that GEOV2 products keep a high consistency with GEOV1 (90% of residuals within ± max (0.5, 20%) LAI, and 80% within ± max(0.05, 10%) FAPAR / FCover) and improves in terms of product completeness (<1% of missing data), temporal consistency, consistency across variables and accuracy.

1. Introduction

Vegetation state and dynamics play a key role in the global climate and biochemical cycles. The leaf area index (LAI) and the fraction of absorbed photosynthetic active radiation (FAPAR) are essential climate variables (GCOS, 2022) intervening within key processes, including photosynthesis, respiration and transpiration. These vegetation variables control the exchanges between the biosphere and the atmosphere, and they are crucial in several applications from climate and land surface modelling at the global scale to agricultural and forest management at the landscape scale (Fang et al., 2019a). The fraction of green vegetation cover (FCover) as seen from nadir is also crucial for partitioning contributions between soil and vegetation in land surface models.

Over the last two decades, several LAI, FAPAR and FCover global datasets have been routinely produced from moderate resolution satellite data including MODIS (Myneni et al., 2002), VIIRS (Yan et al., 2018), VEGETATION (VGT) (Baret et al., 2007) or OLCI (Gobron, 2011) among others (see a review in Bayat et al. (2021)). At the European level, the Copernicus Global Land Service (CGLS) provided Version 1 of Collection 1 km LAI, FAPAR and FCover products, also known as GEOV1, derived from SPOT/VGT and PROBA-V data for the 1999–2020 period products (Baret et al., 2013). GEOV1 products were delivered every 10 days with a 12-day lag. Validation studies showed that GEOV1 outperformed other existing products both in terms of accuracy and precision (Camacho et al., 2013). While being one of the smoothest available products, GEOV1 displayed some temporal inconsistencies and noise mainly caused by cloud contamination, residual atmospheric or directional effects, and snow cover. More importantly, this product exhibited a significant fraction of missing data specifically due to snow for high-latitude canopies and cloud cover for tropical forests. Intercomparison exercises confirmed that the existing global moderate resolution biophysical products including GEOV1 do not meet GCOS and CGLS user requirements (CGLS, 2015) in terms of temporal consistency, stability, continuity and uncertainty, particularly for tropical and boreal regions (Camacho et al., 2013; Fang et al., 2013; Jin et al., 2017). To comply with the CGLS user requirements (CGLS, 2015), Version 2 of CGLS 1 km products, hereafter GEOV2, were designed to be consistent with GEOV1 while improving their limitations in terms of continuity and

* Corresponding author at: CIDE, CSIC-UV-GVA, 46113 València, Spain.
E-mail address: verger@csic.es (A. Verger).

https://doi.org/10.1016/j.jag.2023.103479
Received 30 June 2023; Received in revised form 16 August 2023; Accepted 2 September 2023
Available online 9 September 2023

smoothness and providing near real time estimates with a maximum of 2-day lag.

Both GEOV1 and GEOV2 capitalize on the development and validation of already existing products, and the use of machine learning techniques (Baret et al., 2013; Verger et al., 2008; Verrelst et al., 2012). The main difference between GEOV1 and GEOV2 is the temporal composition approach used to generate products at a 10-day step. Temporal compositing highly determines the temporal stability and continuity of the derived satellite biophysical products (Huang et al., 2021; Verger et al., 2016). The LAI retrieval algorithms adopt a wide variety of temporal approaches. This includes the well-known maximum value compositing used in MODIS algorithm (Myneni et al., 2002). This compositing strategy operates over a local temporal window and cannot take full advantage of the temporal correlation of the observations which can also be informative (Pu et al., 2023). The temporal correlation information is used in GEOV1 algorithm which incorporates temporal prior knowledge to better constraint a kernel driven model inversion for the bidirectional reflectance distribution function (BRDF) within a temporal weighted 30-day compositing window (Baret et al., 2007; Baret et al., 2013). However, this compositing approach is limited by the realism of the BRDF model, and it may induce inconsistent retrievals at extreme sun angles, particularly, at high latitudes during the wintertime (Verger et al., 2015). In addition, this compositing technique cannot deal with long periods of missing data due to permanent cloud or snow cover within the 30-day compositing window which results in poor temporal continuity in the GEOV1 products (Camacho et al., 2013). More elaborated methods were designed to smooth time series, fill gaps and to provide short term forecast using temporal prior information over a long period, combined with daily product values. Verger et al. (2013) derived LAI at 10-day frequency by fitting a phenology model based on the climatology (i.e. the inter-annual mean of long-term time series of LAI) to the daily estimates over each season. This climatological fitting approach is superior to standard reconstruction methods in situations with long periods of missing data (Kandasamy et al., 2013; Verger et al., 2013). Conversely, a local asymmetric Savitzky-Golay filter using linear interpolation for gap filling over a limited temporal window of 120 days as proposed by Verger et al. (2011) improved the accuracy of the of LAI time series with a gap fraction up to 60% (Kandasamy et al., 2013). These previous studies inspired us to develop a smoothing and gap filling approach where the temporal prior information derived from the exploitation of the several years available in the time series could be used more explicitly in a temporal technique working over a limited local time window. These principles were exploited in GEOV2. A climatology is ingested as a background information for improving the reliability of a local polynomial compositing method. Further, similar to MODIS principles, a maximum envelope approach is used to filter outliers and improve the accuracy and stability of retrievals.

This paper describes the GEOV2 algorithm and the resulting LAI, FAPAR and FCover products derived from SPOT/VGT (1999–2013) and PROBA-V (2014–2020) data. GEOV2 products will be evaluated based on the comparison with GEOV1 and MODIS products, as well as with ground measurements. We focus here in the processing of the historical time series for 1999–2020 period, as the near real time algorithm was already described and evaluated in Verger et al. (2014).

2. Material and methods

2.1. GEOV2 algorithm description

We describe here the principles of GEOV2 retrieval algorithm.

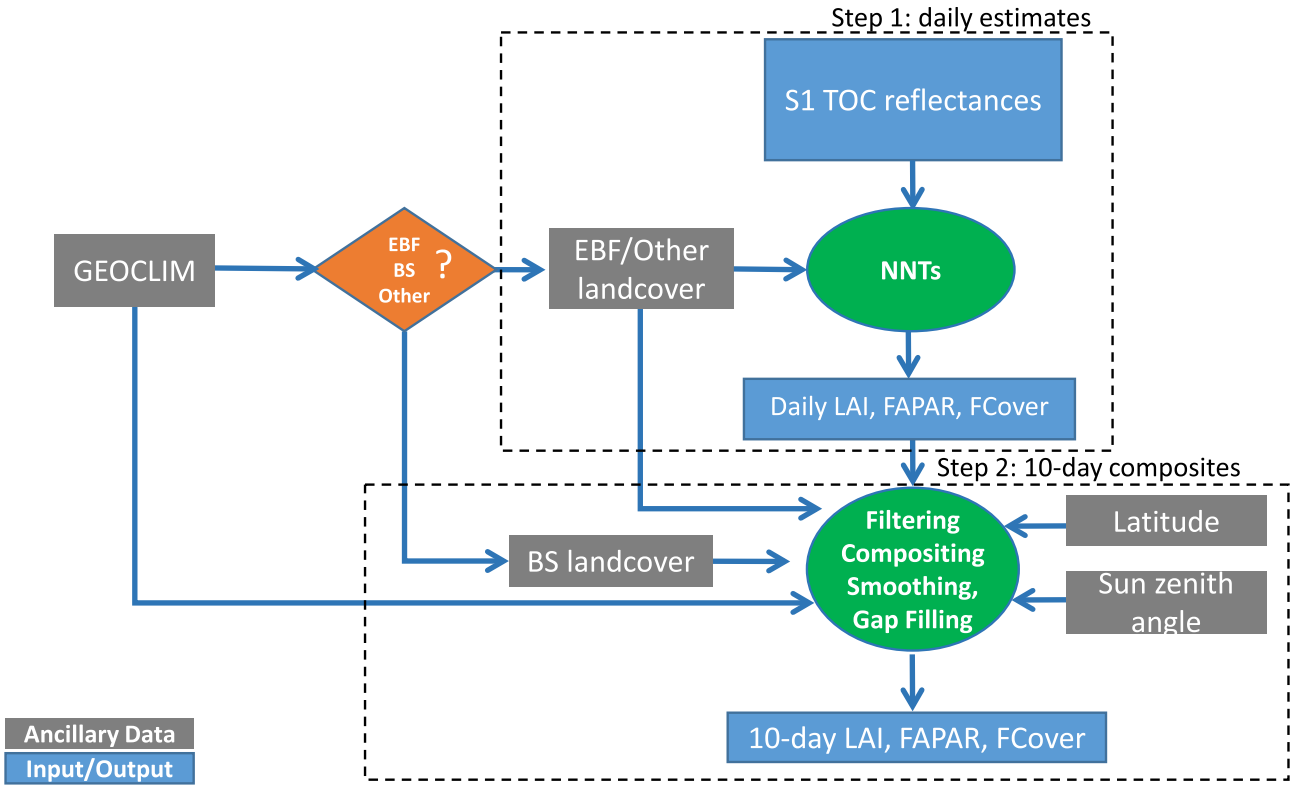

Fig. 1. Flow chart of GEOV2 retrieval algorithm. In step 1, daily synthesis (S1) top of canopy (TOC) reflectance from SPOT/VGT and PROBA-V are transformed into daily estimates of LAI, FAPAR and FCover using two neural networks (NNTs) specifically trained for Evergreen Broadleaf Forest (EBF) and non EBF pixels. In step 2, dedicated filtering, smoothing, gap filling and compositing temporal techniques are applied. The inputs of this second step are the daily estimates (S1), the sun zenith angle of the observations, the latitude, a climatology of LAI, FAPAR and FCover (GEOCLIM), and the EBF and Bare Soil (BS) landcover classes derived from GEOCLIM. The outputs are the final 10-day LAI, FAPAR and FCover GEOV2 products.

Further details are provided in the algorithm theoretical basis document (https://land.copernicus.eu/global/documents/products). The algorithm consists of two main steps (Fig. 1): (1) neural networks first compute daily LAI, FAPAR and FCover estimates from SPOT/VGT and PROBA-V data; (2) the daily LAI, FAPAR and FCover estimates were then composited every 10-day.

2.1.1. Daily LAI, FAPAR, and FCover estimates

The derivation of the biophysical daily estimates of LAI, FAPAR and FCover is based on the application of neural networks trained over existing Carbon cYcle and Change in Land Observational Products from an Ensemble of Satellites (CYCLOPES) version 3.1 (Baret et al., 2007) and MODIS Collection 5 (Yang et al., 2006) like in GEOV1 algorithm (Baret et al., 2013) and as demonstrated first by Verger et al. (2008). To be consistent with GEOV1, the neural networks were trained using VGT input data. The inputs are top of the canopy daily S1 reflectance in red, near infrared (NIR) and short-wave infrared (SWIR) spectral bands (Fig. S1), and the cosine of the three associated sun-view angles (view zenith, sun zenith and relative azimuth angles). The corresponding target biophysical variables were coming from the fusion between CYCLOPES and MODIS. Since previous validation studies (e.g. Camacho et al., 2013) demonstrated that MODIS overestimated low LAI/FAPAR values whilst CYCLOPES showed an earlier saturation for high values, the fusion (Table 1) aimed to mitigate the limitations of individual products and combining them to take advantage of CYCLOPES products for low LAI/FAPAR values and MODIS for high LAI/FAPAR values, respectively (Verger et al., 2014). Note that for FCover, no fusion was completed since CYCLOPES was the only available source product.

The training was achieved for the 2003–2007 period over the BELMANIP2.1 (Weiss et al., 2014) set of sites. Two sets of specific neural networks, one for Evergreen Broadleaf Forests (EBF) and one for non-EBF, were calibrated for each of the three variables: LAI, FAPAR and FCover (Fig. S2). EBF identification corresponds to the EBF/non-EBF classification of the GEOCLIM dataset, based on the magnitude and seasonality of GEOV1 LAI time series (Verger et al., 2015). Since the neural networks were trained on VGT reflectance data, we applied a bandpass adjustment to PROBA-V (2014–2020) to get VGT like TOC reflectance and rescaled the PROBA-V neural network estimates to VGT ones.

2.1.2. Generation of 10-day composites

To get continuous and consistent time series the daily LAI, FAPAR and FCover estimates were composited every 10-day (Fig. 2, Fig. S3). First, for pixels identified as EBF (Fig. S4b) and for high latitudes ($lat > 55^{\circ}$) in winter time (sun zenith angle, $SZA > 70^{\circ}$) the outliers are filtered assuming a small seasonal amplitude and, respectively, high (Fig. 3a) and low values of LAI (Fig. 3b, c) (Verger et al., 2015). Then, the Consistent Adjustment of Climatology to Actual Observations (CACAO) (Verger et al., 2013) technique and Temporal Smoothing Gap Filling (TSGF) Savitzky-Golay based filter (Verger et al., 2011) were applied (Fig. 2). CACAO consists of fitting a climatology to the daily estimates by adjusting the magnitude and shifting the climatology in time for each season (Verger et al., 2013). We used GEOCLIM (Verger et al., 2015) as the climatology (dashed green line in Fig. 3). The resulting CACAO values (continuous green line in Fig. 3) are evenly distributed every 10-days, and then used to fill gaps before the application of TSGF if less than six daily estimates exist in a 60-day semi-window. TSGF fits a weighted second-degree polynomial over an asymmetric temporal window. The compositing window is made of semi-windows at each side of the date of the product with an adaptive length varying between 15 and 60 days that contains at least six valid daily estimates or CACAO values the closest to the date at which the product is generated (Verger et al., 2014). This process is repeated three times (Fig. 2) and the daily estimates are filtered and weighted based on their distance Δ to the TSGF composites computed in the previous iteration using an upper envelope approach with weights defined as $W = 2/(1+\exp(-2^{*}\Delta))$ which assigns less weight to the lower values than TSGF since they are affected by cloud contamination (Cihlar, 1996). In the first iteration W were fixed to 1. To put less emphasis on the climatological values used to fill gaps, weights of CACAO values were multiplied by a scale factor of 0.5. Finally, when the climatology is not available, the residual gaps are filled using a linear interpolation within a $\pm$ 60-day window. Gaps longer than 120 days are not filled and are flagged as missing data. The products are provided with several quality indicators (Fig. S4) and the pathway used to fill the possible gaps is also indicated.

2.2. Other satellite products

2.2.1. GEOV1 and differences with GEOV2

We used the GEOV1 LAI, FAPAR and FCover products (Baret et al., 2013) which, as GEOV2, are available over plate carrée projection at 1/112° spatial resolution and a temporal step of 10 days on the CGLS web site (https://land.copernicus.eu/global/products). Both GEOV1 and GEOV2 are derived from SPOT/VGT and PROBA-V data. And they are based on neural networks calibrated with CYCLOPES and MODIS products. However, some differences in algorithms exist between GEOV1 and GEOV2 (Table 1).

2.2.2. MODIS

We used the TERRA MODIS C6 LAI and FAPAR products (MOD15A2H), which are available at a spatial resolution of 500 m over

Table 1
Algorithm differences between GEOV1 and GEOV2.

	GEOV1	GEOV2
Neural network (NNTs) inputs	30-day directionally normalized top of the canopy reflectance composites every 10 days (nadir) in the red, NIR and SWIR bands	Top of canopy daily bidirectional reflectance in the red, NIR and SWIR bands
	Cosine of median sun zenith angle of observations in the compositing period which is used for normalization	Cosine of the zenith and relative azimuth angles of sun and view directions
Weighting function for CYCLOPES and MODIS fusion (NNTs training)	$\begin{cases} LAI_{fused} = LAI_{MODC5}.(1-w) + LAI_{CYCV31} \bullet w \\ fAPAR_{fused} = fAPAR_{MODC5} \bullet (1-w) + fAPAR_{CYCV31} \bullet w \end{cases}$	
	$w = min(1, \frac{1}{4} LAI_{CYCV31})$	$w = \frac{1}{0.982}(1 - \frac{1}{(1+\exp(-2.LAI_{CYCV31}+4))})$
Training & application of NNTs	Generic	Specific: evergreen broadleaf forest (EBF) and non-EBF distinction
Temporal composition	Composition of input reflectance based on a 15-day semi-period with Gaussian weighting	Composition of the output daily biophysical estimates using an adaptive temporal window. The length of each semi-period varies between 15 and 60 days so that it contains at least 6 valid observations
Temporal smoothing and gap filling	Not applied	Application of Temporal Smoothing and Gap Filling (TSGF) and Consistent Adjustment of Climatology to Actual Observations (CACAO) filters
Near Real Time	12-day lag delivery	2-day lag delivery

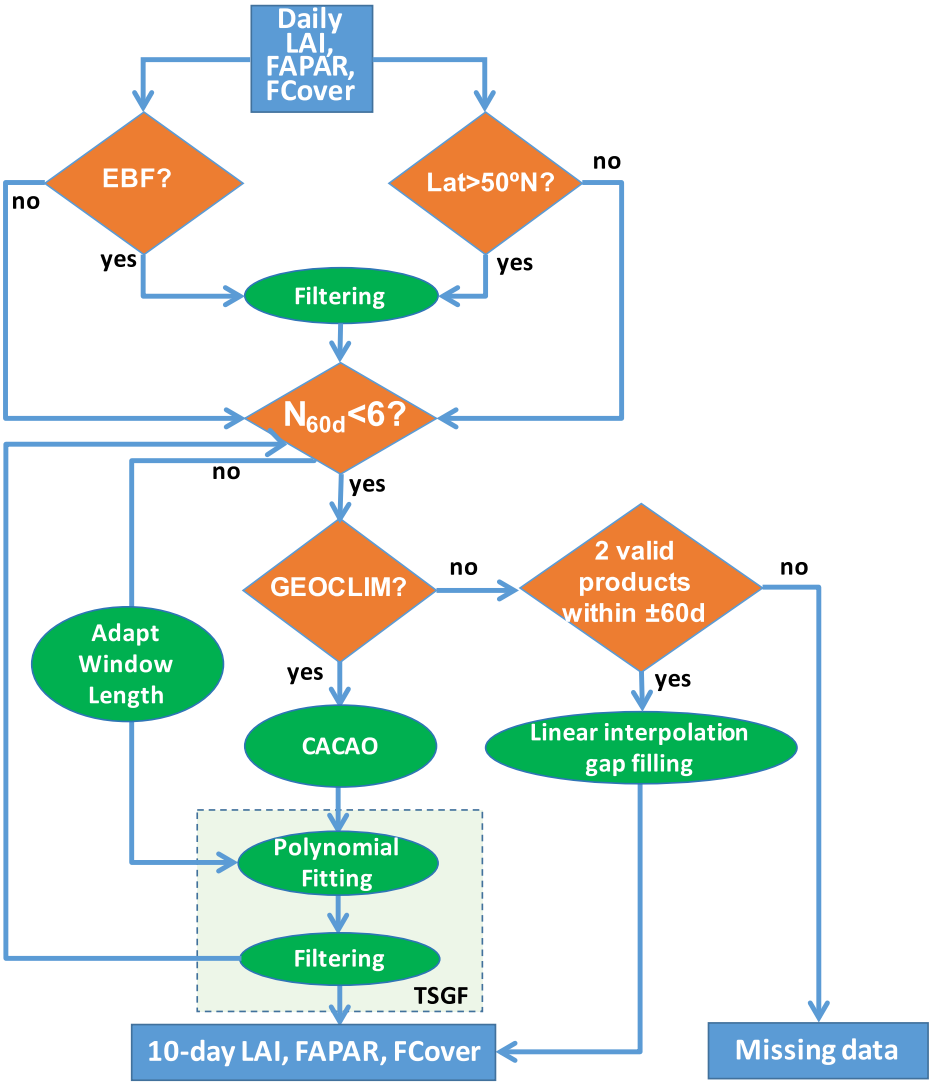

Fig. 2. Flowchart for the generation of 10-day composites: filtering, smoothing and gap filling time series depends on the number of available observations within ± 60 days (N_{60d}).

a sinusoidal grid and a step of eight days since 2000 at https://ladsweb.modaps.eosdis.nasa.gov. The main retrieval algorithm is based on the inversion of a 3D radiative transfer model using a look-up table which depends on the landcover (Yan et al., 2016). The MOD15A2H products were reprojected and resampled to the GEOV2 grid. The quality flag was used to retain only the best quality values.

2.3. Assessing the quality of the GEOV2 products

The validation approach follows the CEOS land product validation guidelines (Fernandes et al., 2014):

- **Product completeness**: spatio-temporal continuity of the products.
- **Temporal consistency**: We assessed the seasonality of typical temporal profiles of different biome types during the 2012–2015 period.
- **Spatial consistency**: We assessed the consistency between SPOT/VGT and PROBA-V GEOV2 products during the overlapping period of the two sensors from October 2013 to March 2014. We also compared GEOV2 with GEOV1 and MODIS C6 products during the 2012–2015 period. GEOV2 (product Y) and the reference product (X) are spatially consistent when their residuals (ε), computed as $\varepsilon = Y-(aX+b)$ where a and b result from the linear fit between the two products, are within the optimal uncertainty levels of the variables defined as max(0.5, 20%) for LAI and max(0.05, 10%) for FAPAR and FCover. These levels correspond to the CGLS (2015) and GCOS (2011) accuracy requirements for LAI and FAPAR.
- **Statistical analysis** between products: We compared GEOV2 products derived from SPOT/VGT with those from PROBA-V, GEOV1 and MODIS C6 products of the closest date over 3 km × 3 km support area over the LANDVAL sites (https://calvalportal.ceos.org/sampling) (Fuster et al., 2020).
- **Accuracy assessment**: We validated GEOV2, GEOV1 and MODIS products against the ground measurements available in the DIRECT2.0 (http://calvalportal.ceos.org/web/olive/site-description) database during the 2000–2017 period. The comparison was performed at 3 km × 3 km. The closest satellite product date to the field campaign within a maximum period of ± 15 days was used.

3. Results

A selection of main validation results is presented here. For additional quality evaluation results the reader can refer to the GEOV2 validation reports (https://land.copernicus.eu/global/documents/products).

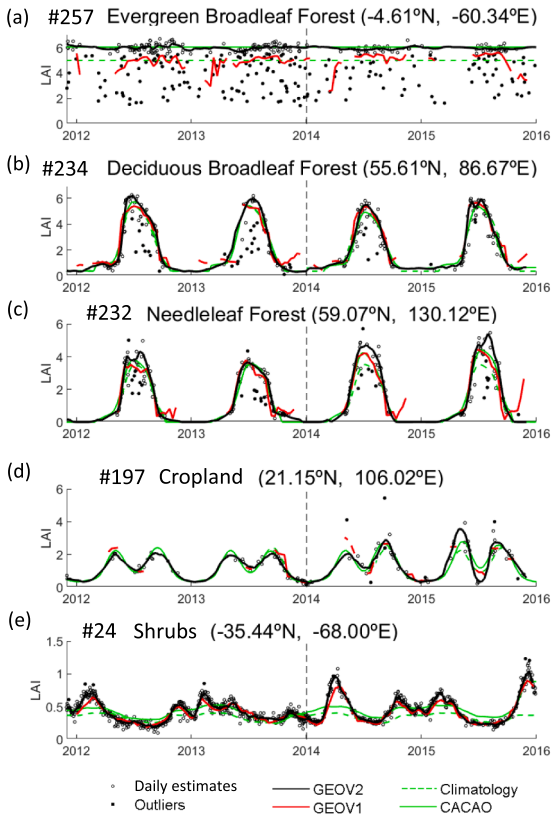

Fig. 3. Temporal profile of GEOV2 LAI product (black solid line) for the 2012–2015 period over a selection of LANDVAL sites. The site number, biome type and location are indicated. The dashed black line indicates the switchover from SPOT/VGT to PROBA-V. Empty dots correspond to the daily valid LAI estimates and filled dots to the outliers. The red line corresponds to GEOV1. The dashed green line corresponds to the climatology derived from GEOV1 1999–2010 time series (GEOCLIM). The solid green line to the CACAO estimates: the climatology adapted to the daily estimates.

3.1. Completeness

GEOV2 highly improved product completeness as compared to GEOV1. It shows<1% of missing values at the global scale (Fig. S3), only at very high latitudes where GEOCLIM climatology was not available (Verger et al., 2015). The percentage of filled land pixels in GEOV2 is very similar to the percentage of missing values in GEOV1 (Fig. 4). The lack of PROBA-V satellite observations goes up to 80% over large regions in the northern latitudes (Fig. 4a) mainly due to snow cover or cloudiness in wintertime (Fig. 4c) and over equatorial regions (Fig. 4a) with persistent cloud coverage (Fig. 4c) and in these cases the climatological gap filling is applied in GEOV2. The percentages of filled pixels for GEOV2 are greater than the percentage of missing values for GEOV1 in EBF areas as well as for deciduous broadleaf and mixed forests in summer (cf. Fig. 4c-d) because, in these cases, a high fraction of data with residual cloud cover is filtered out in the outlier rejection process applied in GEOV2 (Fig. 3, a, b, c) but, even in these cases, the final product shows full spatio-temporal continuity (Fig. S3).

3.2. Temporal consistency

The analysis of the temporal consistency per biome type shows (Fig. 3):

- For EBF (Fig. 3a), the effect of residual clouds is very pronounced, creating strongly negative biased estimates of the daily products. These outliers are filtered and GEOV2 shows a low seasonality with a high level of LAI as expected. As compared to GEOV2, GEOV1 shows generally lower LAI values, discontinuous and shaky temporal profiles.
- For deciduous broadleaf forest (Fig. 3b), the negatively biased daily estimates affected by cloud contamination (Cihlar, 1996) are efficiently filtered by the upper envelope approach in the GEOV2 algorithm.
- For very high northern latitude needleleaf forests (Fig. 3c), the GEOV2 temporal profile is consistent with that of GEOV1 during the growing season, while no interruption is observed during the winter period conversely to GEOV1. Further, GEOV2 corrects the

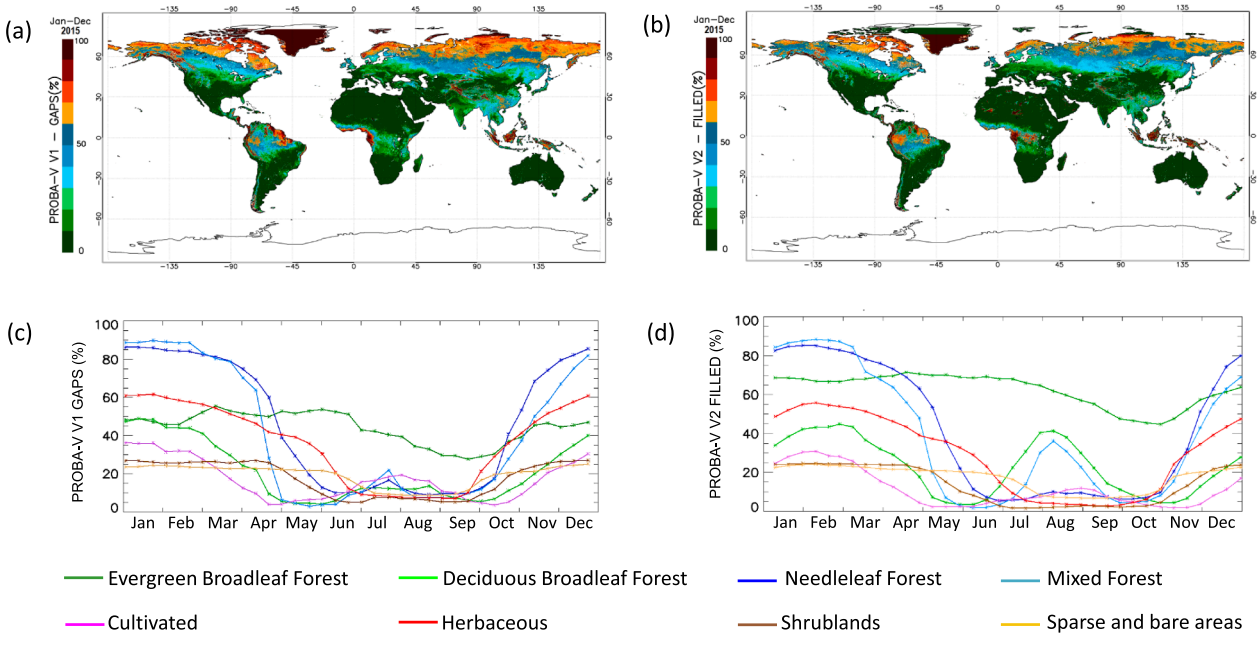

Fig. 4. GEOV1 and GEOV2 product completeness. Percentage of missing values for GEOV1 products (left) and percentage of filled land pixels for GEOV2 products (right): maps of average values over year 2015 (top) and temporal evolution per biome (Buchhorn et al., 2020) (bottom).

anomalous high values in winter time observed in GEOV1 due to snow or directional effects under extreme illumination conditions that limit the reliability of the BRDF model (Roujean et al., 1992) applied in GEOV1.
- The seasonality of the double cycle cropland (Fig. 3d) is consistently described by both GEOV1 and GEOV2. However, the discontinuities noticed for GEOV1 have disappeared in GEOV2.
- The temporal profile of the shrubland (Fig. 3e) is well captured by both GEOV1 and GEOV2.

These results show that GEOV2 largely improves as compared to GEOV1, both in terms of temporal smoothness (Fig. S5) and temporal continuity (no gaps). Further, GEOV2 shows a smooth transition between SPOT/VGT and PROBA-V (Fig. 3).

3.3. Spatial consistency

3.3.1. Consistency between SPOT/VGT and PROBA-V estimates

Overall, PROBA-V and SPOT/VGT GEOV2 products are spatially consistent (Fig. 5a), with histograms of residuals (Fig. 5b) showing narrow distributions centred at zero with more than 95% of residuals ranging between ± 0.5 LAI, and around 90% within ± 0.05 FAPAR and FCover (Fig. S6). The highest spatial inconsistencies are observed in the South hemisphere regions (EBF in Africa and cultivated areas in South of America) that show the highest vegetation activity during the overlapping period between PROBA-V and SPOT/VGT (Fig. S3). In these cases, PROBA-V systematically provides higher values than SPOT/VGT (Fig. S7). These inconsistencies are due, in part, to the differences in the spectral response function (Fig. S1), point spread function and processing chain (e.g., cloud-aerosol screening) of input TOC reflectance between sensors.

3.3.2. Consistency between GEOV1 and GEOV2 products

GEOV2 and GEOV1 are spatially consistent with 90% (80%) of residuals within the CGLS uncertainty requirements for LAI (FAPAR and FCover) (Fig. 6). The highest spatial inconsistencies are observed over Equatorial Areas and Northern high latitudes. For EBF pixels, GEOV2 shows higher LAI, FAPAR and FCover values than GEOV1 (Fig. S8). In northern high latitudes positive residuals (up to 1 LAI and 0.1 FAPAR and FCover) are also observed in summer when the vegetation activity and development is at its maximum (Fig. S8, b, d, f) whilst negative residuals in winter period when, if available, GEOV1 provides unrealistic high values (Fig. S8, a, c, e; Fig. 3, b, c). For FCover (Fig. 6e), some spatial inconsistencies are observed over Sahara Desert corresponding to a false seasonality depicted in GEOV1 which is corrected in GEOV2 (Fig. S3).

3.3.3. Consistency between GEOV2 and MODIS C6 products

MODIS C6 products shows higher spatial inconsistencies with GEOV2 than GEOV1 (Fig. 7, Fig. S9): 75% of LAI residuals are matching the accuracy requirements but only 50% for FAPAR. The histograms of FAPAR residuals per month are slightly biased towards negative values, centered around −0.03 (Fig. 7d). MODIS shows higher FAPAR values than GEOV2 over sparsely vegetated regions and over widespread areas during the vegetation dormancy (Fig. S9 c, d).

3.4. Statistical analysis

The scatterplots between PROBA-V and SPOT/VGT GEOV2 over the LANDVAL sites during the overlapping period (2013/10/16——2014/03/31) show that the two products agree well (RMSD < 0.2 for LAI and < 0.03 for FAPAR and FCover). Additionally, the relationship is unbiased (Fig. 8a-c).

GEOV2 and GEOV1 LAI products show very good consistency for LAI lower than 4 (Fig. 8d). For larger values of LAI, there is higher scattering between GEOV2 and GEOV1 and a systematic bias partially due to the noise in the data and to the different processing applied to EBF pixels for the two versions. GEOV1 is lower than GEOV2 for EBF pixels and produced wider distributions of LAI (Fig. S10). Indeed, it is more affected by noise and shows a negative bias due to cloud misdetections as compared to GEOV2 (Fig. 3a) which benefits from an improved cloud filtering and smoothing. The overall RMSD across biomes is 0.47 (33%) LAI with very high correlation between GEOV2 and GEOV1 (R = 0.97). For FAPAR (Fig. 8e, Fig. S11) and FCover (Fig. 8f, Fig. S12) variables very strong consistency (R = 0.98, RMSD < 0.07 (18%)) is also observed between GEOV2 and GEOV1. Note however that GEOV2 values are slightly lower than GEOV1 for FAPAR values ranging between 0.25 and 0.85 (Fig. 8e), and FCover close to 1 (Fig. 8f, Fig. S12). GEOV2 allows to partially correct the systematic overestimation of GEOV1 FAPAR and FCover values observed against ground measurements (Fuster et al. (2020); c.f. section 3.5).

The comparison between GEOV2 and MODIS C6 LAI products (Fig. 8g) shows a good agreement with, however, a higher scattering and GEOV2 systematically providing higher estimates than MODIS intermediate LAI values. The high scattering is partially associated to the noise in MODIS product which is characterized by having low stability (Fig. S5) (Camacho et al., 2013). For FAPAR, GEOV2 and MODIS C6 highly agree (Fig. 8h, S11) except for low values where MODIS FAPAR shows a positive bias which is a well-recognized issue: MODIS FAPAR overestimates low FAPAR values over sparsely vegetated areas (Camacho et al., 2013; McCallum et al., 2010; Steinberg et al., 2006).

3.5. Accuracy assessment

GEOV2 correlates the best with DIRECT2.0 ground measurements of LAI, FAPAR and FCover (Fig. 9). GEOV2 and GEOV1 LAI show similar accuracies: RMSD of 0.91 and 0.85, respectively, and are slightly better than MODIS C6 (RMSD of 1.03 LAI). GEOV2 FAPAR and FCover slightly improves the accuracy of GEOV1: RMSD of 0.11 FAPAR and 0.15 FCover for GEOV2 in comparison with 0.12 FAPAR and 0.17 FCover for GEOV1.

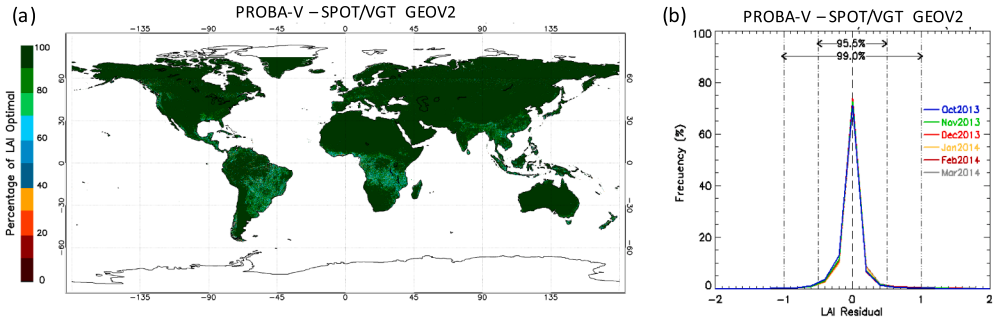

Fig. 5. Consistency between SPOT/VGT and PROBA-V GEOV2 LAI products during the overlapping period from October 2013 to March 2014: (a) Percentage of cases within CGLS optimal uncertainty levels: max(0.5, 20%) LAI; (b) Histogram of residuals per month.

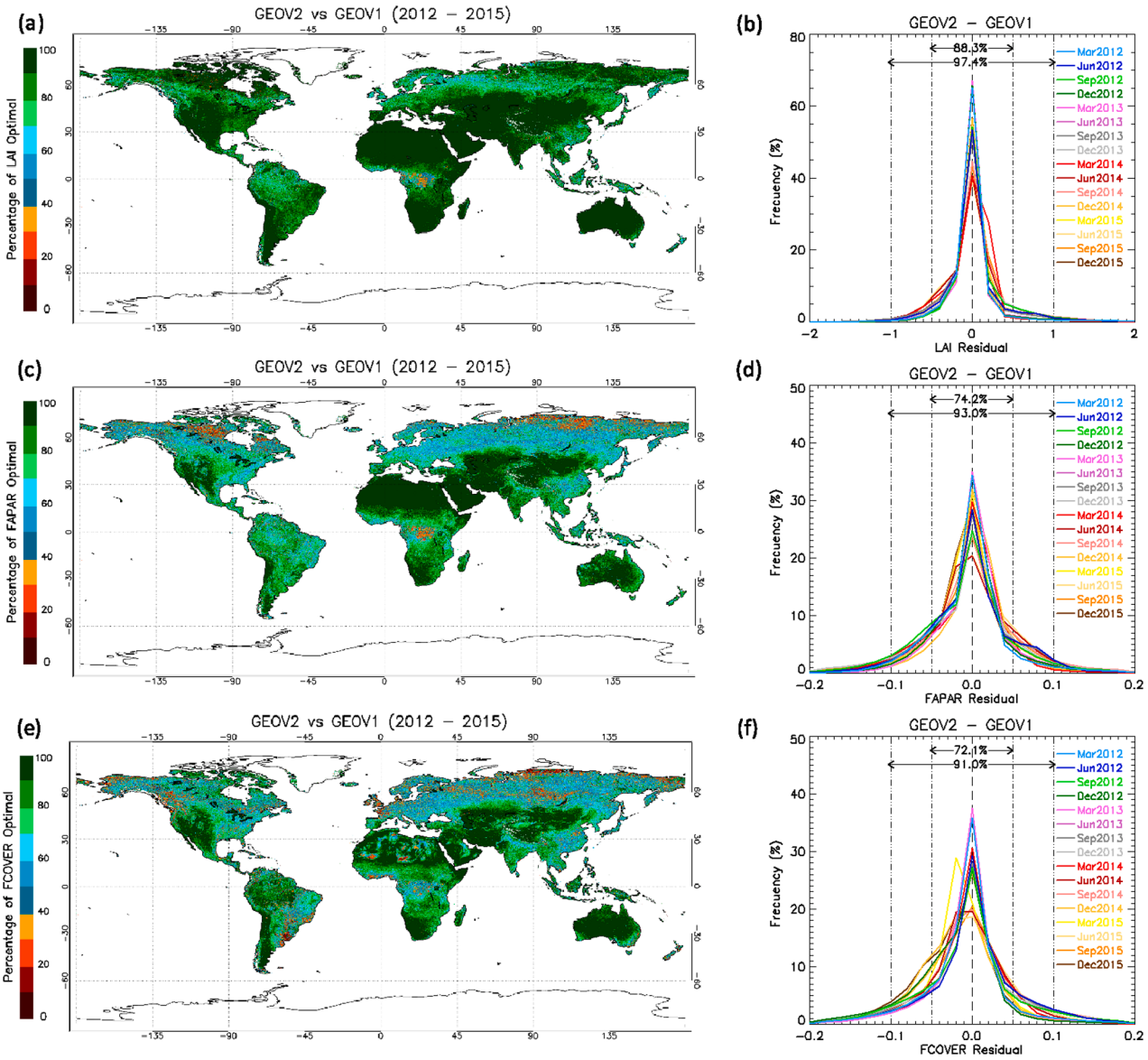

Fig. 6. Consistency between GEOV2 and GEOV1 products during the 2012–2015 period, from top to bottom: LAI, FAPAR and FCover. Left: percentage of cases within CGLS optimal uncertainty levels: max(0.5, 20%) LAI and max(0.05, 10%) FAPAR / FCover. Right: histogram of residuals per month.

However, both GEOV2 and GEOV1 overestimate ground values of FAPAR and FCover with a higher positive bias for GEOV1: mean bias of 0.04 (8%) FAPAR for GEOV2 compared with 0.06 (14%) FAPAR for GEOV1, and bias of 0.08 (18%) FCover for both GEOV2 and GEOV1 with a slope from MAR of 1.18 and 1.27, respectively. GEOV1 and GEOV2 products show better results than MODIS C6 FAPAR (RMSD of 0.15 and bias of 0.06 (12%)) and partially reduce the systematic positive bias for low FAPAR values observed for MODIS.

4. Discussion

GEOV2 products are already widely used for land surface modelling, photosynthesis and gross primary production estimation (Zhang et al., 2020), evapotranspiration estimation (Yin et al., 2021), phenology estimation (Bórnez et al., 2020), drought monitoring (Cammalleri et al., 2019) or crop monitoring (Du et al., 2022), among many other applications. Regardless the application, we highly recommend to the users to pay due attention to the quality indicators associated to the products. We discuss here the limitations of GEOV2 algorithm and derived products.

SPOT/VGT and PROBA-V GEOV2 products are consistent across the overlapping period. However, a long-term trend analysis revealed that sensor shift may have resulted in a spurious increase in LAI and associated uncertainties (Fang et al., 2021b). This may indicate some residual inconsistencies in the input TOC reflectance between PROBA-V and SPOT/VGT which transfer to the GEOV2 time series. The new collection of PROBA-V TOC reflectance (Toté et al., 2021), soon to be released, may contribute to improve GEOV2 times series. Improving their long-term consistency is crucial for a better understanding of the trend of global LAI and the spatio-temporal patterns of carbon sink and source of ecosystems.

GEOV2 highly improves GEOV1 in terms of product completeness (Fig. 4): <1% of missing data for GEOV2 compared to more than 70% and 80% of gaps for GEOV1 in the tropical forests and high latitudes in winter, respectively. If GEOCLIM climatology is available for a given pixel, GEOV2 products have no missing data because the CACAO method allows filling all the gaps in the time series. CACAO, as compared to the original climatology, allows inter-annual variations of the time course and adaptation to actual observations (Fig. 3). However, the main limitation of the CACAO reconstruction method is its inability

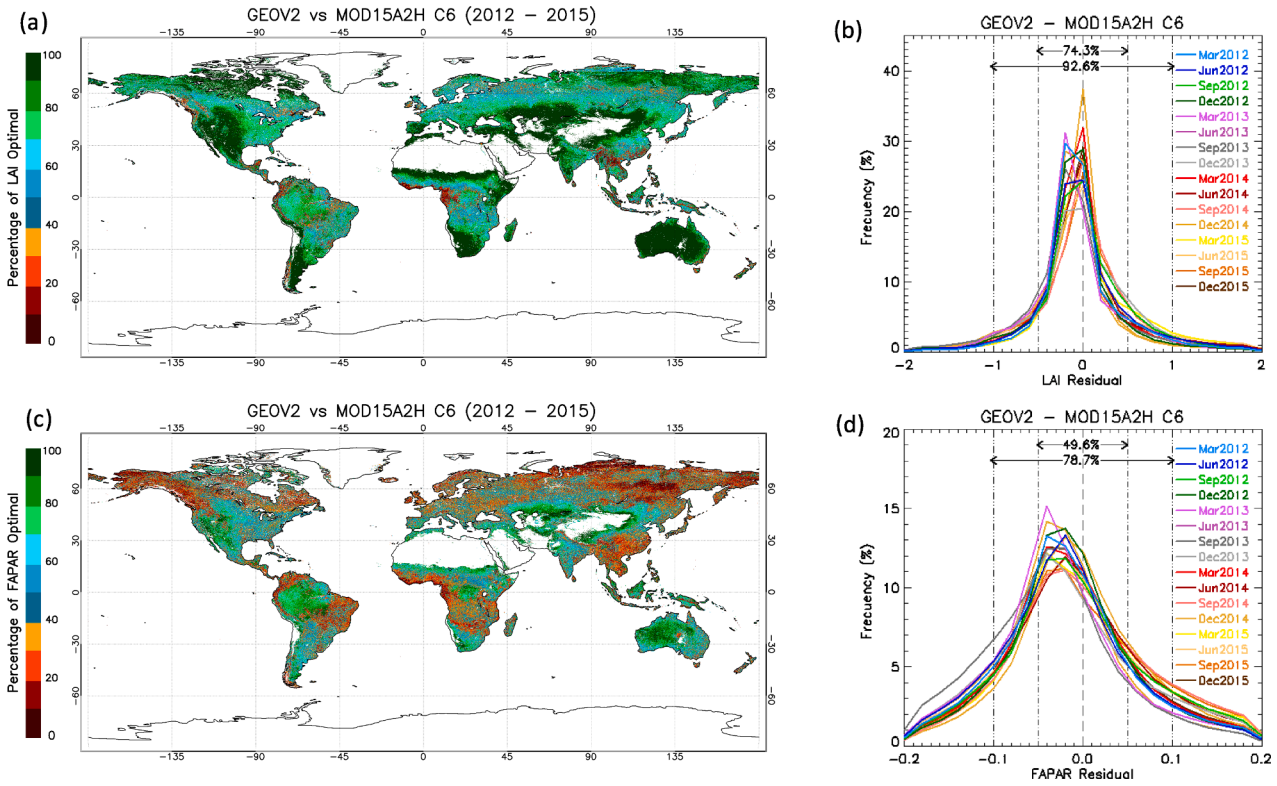

Fig. 7. Consistency between GEOV2 and MODIS C6 products during the 2012–2015 period for LAI (top) and fAPAR (bottom). Left: percentage of cases within CGLS optimal uncertainty levels: max(0.5, 20%) LAI and max(0.05, 10%) FAPAR (left). Right: histogram of residuals per month.

to capture underlying atypical modes of seasonality in the time series that strongly differ from the average climatology (Fig. 3e; Verger et al., 2013). To prevent from such drawback, in GEOV2 algorithm priority is given to TSGF smoothing since it is closer than CACAO to the daily estimates, while CACAO is only used to fill large gaps in the time series. This approach mostly overcomes CACAO limitations, and the final products capture the seasonal abrupt variations in vegetation temporal evolution including land cover changes, flood or fire events (Fig. S13). Recent studies demonstrated the accuracy of the phenology metrics retrieved from GEOV2 products as compared to other satellite products (Yu et al., 2021) and ground-based measurements (Bórnez et al., 2020), which suggest that these smoothed time series correctly replicate the vegetation seasonality.

The GEOV2 algorithm uses a static mask for EBF identification based on GEOCLIM climatology for the period 1999–2010. For pixels flagged as EBF, GEOV2 assumes a low seasonality and only reproduces the high values of the time series but cannot capture disturbances including deforestation processes. A future evolution of GEOV2 products could include an update of the EBF mask with recent time series and auxiliary data, and a dynamic EBF detection.

GEOV2 improved internal consistency between variables as compared to GEOV1 (Fig. S14) which showed few artefacts for low FCover values and inconsistent FAPAR-FCover relationship. This partially contradicts a recent study by Mota et al. (2021) who claimed that GEOV2 LAI and FAPAR products lacked consistency in their spatial and temporal changes. In this sense, they recommend to use the TIP (Pinty et al., 2011) approach which uses their LAI product among other variables to derive FAPAR, allowing, by construction, to keep consistency across variables. However, even though temporal changes in LAI is the primary driver of temporal changes in FAPAR, changes in leaf and canopy properties and environmental conditions also impact LAI and FAPAR relationship (Lee et al., 2023). Further the relationship between FAPAR and LAI is asymptotic (Fig. S14), and, for LAI greater than 3, FAPAR saturates at around 0.8–0.9 and is relatively insensitive to changes in LAI. Fang et al. (2021a) explored the relationship between vegetation biophysical variables and showed consistency between GEOV2 FCOVER product and MODIS C6 LAI except in few situations at northern latitudes higher than 50° where the products have higher uncertainties. Further confrontation with continuous ground measurements are required to assess the realism of these global datasets. Yu et al. (2021) validated several kilometric LAI global products using continuous field measurements of LAINet and showed that GEOV2 well reproduced the reference LAI in terms of magnitude and phenology whilst a TIP based product systematically underestimated high LAI values and showed a temporal mismatch with ground measurements. Song et al. (2021) also validated four LAI products with continuous field measurements and showed that GEOV2 provided the highest accuracy and temporal consistency.

GEOV2 products were not impacted by the degradation effects in MODIS C5 after ~ 2007 (Lyapustin et al., 2014) because the MODIS products were only used for the calibration of GEOV2 algorithm and the calibration was achieved in the period 2003–2007 (section 2.1.1).

GEOV2, as well as other satellite products, are not accurate over the wetlands and flooded areas (Campos-Taberner et al., 2018; Fang et al., 2019b; Fuster et al., 2020). They overestimate LAI, FAPAR and FCover values over rice crops during the early and growing periods of development (Fig. 9) because the decrease in reflectance values due to strong water absorption in paddy rice fields is misinterpreted as a dense vegetation canopy. This is a legacy effect since the CYCLOPES V3.1 and MODIS C5 products used for the calibration of GEOV2 algorithm were developed from physical radiative transfer models which are not applicable over heterogeneous surface partially covered with water (Xu et al., 2020). Further algorithm improvements and/or semiempirical corrections are necessary to improve the global LAI, FAPAR and FCover products over the wetlands and flooded areas.

Further validation and comparison with ground data are required in particular for FCover. The confrontation with DIRECT2 measurements showed that both GEOV1 and GEOV2 FCover have a systematic positive

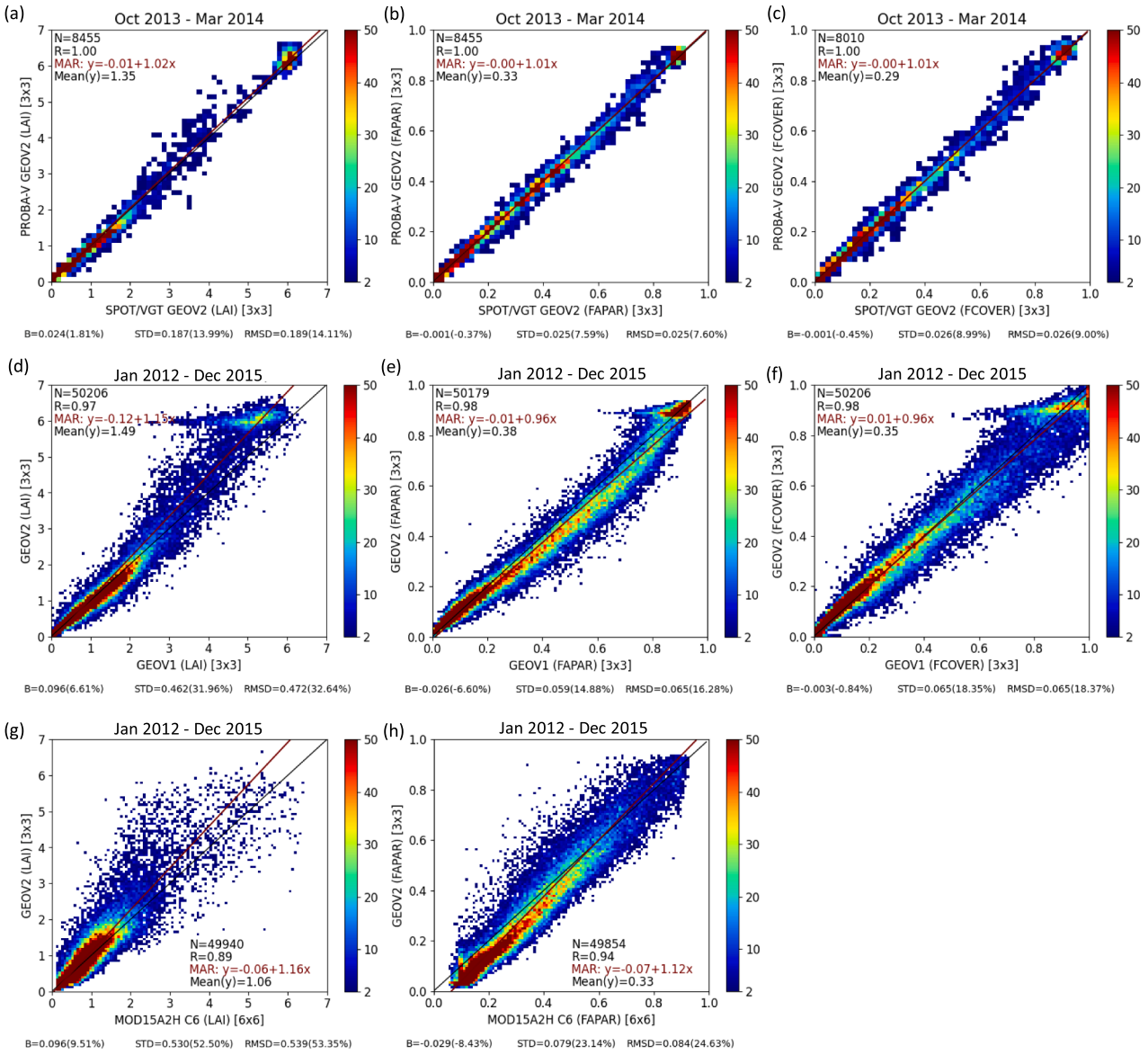

Fig. 8. Scatterplots of concurrent products over the LANDVAL sites between PROBA-V and VGT GEOV2 products during the overlapping 2013–2014 period (top), GEOV2 and GEOV1 (middle), and GEOV2 and MODIS C6 (MOD15A2H, bottom) during 2012–2015: LAI (left), FAPAR (middle) and FCover (right). The comparison is performed at 3 km × 3 km: i.e. 3x3 GEOV1/2 pixels, and 6x6 MODIS pixels. The black line corresponds to the 1:1 line and the continuous red line to the linear fit using major axis regression (MAR). The number of samples (N = sites × dates), the correlation coefficient (R), the offset and slope of the MAR linear regression, the root mean square deviation (RMSD), the bias (B) and the standard deviation (STD) are indicated.

bias for intermediate values despite it is partially reduced for GEOV2 (Fig. 9 c, f). Note however that the accuracy of ground based FCover estimates is partially compromised by the very limited footprint, low spatial resolution and sensitivity to exposure setting of traditional fish-eye cameras which result in an underestimation of intermediate FCover ground-based estimates (Yin et al., 2022).

The proposed algorithm can be adapted to any sensor. These principles have also been applied to AVHRR data to generate long-term LAI, FAPAR and FCover data records for the last four decades since 1981 (Verger et al., 2020) to support studies of long-term global vegetation change.

5. Conclusions

This paper presented the GEOV2 algorithm implemented operationally in the Copernicus Global Land Service (CGLS) for the generation of LAI, FAPAR and FCover Collection 1 km V2 products derived from SPOT/VGT and PROBA-V data at global scale from January 1999 to June 2020 at 1/112° spatial resolution and 10-day frequency. The GEOV2 products are generated in two steps. The first step is based on neural networks trained on a combination of the existing CYCLOPES and MODIS products, that generate daily LAI, FAPAR and FCover estimates. The second step uses dedicated temporal smoothing and gap filling techniques to provide the final 10-day products and ensure consistency and continuity in the time series.

We assessed the quality of GEOV2 products with due attention to the consistency and improvements with GEOV1. GEOV2 products are consistent with GEOV1 at the global scale and meet CGLS and GCOS uncertainty requirements in 90% of cases for LAI, and 80% for FAPAR and FCover. GEOV2 showed a similar accuracy as GEOV1 for LAI and slight improvements for FAPAR and FCover as evaluated over the limited ground measurements available. In addition, GEOV2 highly improves GEOV1 in terms of product completeness and does not show any missing data thanks to climatological gap filling that ensures

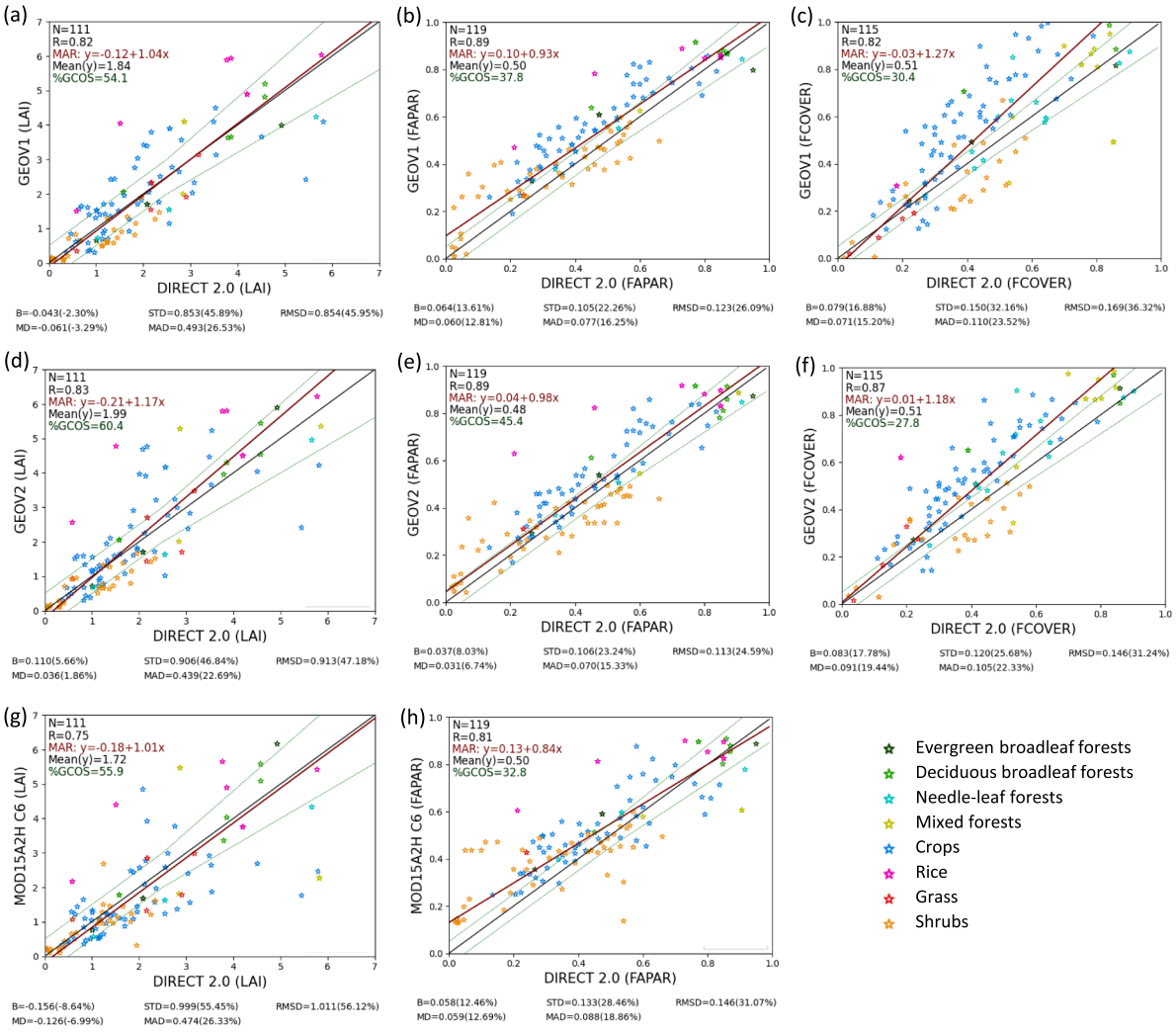

Fig. 9. Comparison between GEOV1 (top), GEOV2 (middle) and MODIS C6 (MCD15A2H, bottom) products with DIRECT2.0 ground-based maps of LAI (left), FAPAR (middle) and FCover (right) over the common samples during the 2000–2017 period. The black line corresponds to the 1:1 line, the dotted green lines to the GCOS and CGLS uncertainty requirements (max(0.5, 20%) for LAI, max(0.05, 10%) for FAPAR for FCover), and the continuous red line to the linear fit using major axis regression.

product retrieval even when scarce or no observation are available during a long period. GEOV2 and GEOV1 time series showed high temporal consistency in most of the situations. GEOV2 corrects the inconsistencies identified in GEOV1 at very high Northern latitudes (artifacts introduced by the BRDF model in extreme illumination conditions) and for evergreen broadleaf forest (noise and discontinuities in GEOV1 due to cloud cover). Additionally, GEOV2 improves both the inter- and intra-annual precision. GEOV2 also improves the internal consistency across variables and corrects both the scattering and some artifacts in the relationships between LAI-FAPAR-FCover.

The SPOT/VGT and PROBA-V GEOV2 LAI, FAPAR and FCover products are available at CGLS portal (https://land.copernicus.eu/global/products). They are used to support a wide range of applications and policies requiring information of the status and evolution of vegetation at global scale.

CRediT authorship contribution statement

Aleixandre Verger: Conceptualization, Methodology, Algorithm development, Software development, Formal analysis, Writing – original draft, Funding acquisition, Writing – review & editing. **Jorge Sánchez-Zapero:** Software development, Validation, Formal analysis, Writing – review & editing. **Marie Weiss:** Conceptualization, Algorithm development, Writing – review & editing. **Adrià Descals:** Software development, Writing – review & editing. **Fernando Camacho:** Validation, Funding acquisition, Writing – review & editing. **Roselyne Lacaze:** Supervision, Scientific project coordination, Funding acquisition, Writing – review & editing. **Frédéric Baret:** Conceptualization, Algorithm development, Supervision, Writing – review & editing.

Declaration of Competing Interest

The authors declare that they have no known competing financial interests or personal relationships that could have appeared to influence the work reported in this paper.

Data availability

The GEOV2 and GEOV1 products are available at the Copernicus Global Land Service data portal (https://land.copernicus.eu/global/products). The MOD15A2H products are available at https://ladsweb.modaps.eosdis.nasa.gov. The DIRECT2.0 reference dataset is available at http://calvalportal.ceos.org/web/olive/site-description.

Acknowledgments

This research was supported by the European Commission through the Framework Service contract no. 199494-JRC and the 7th Framework Programme for Research under grant agreement no. 218795 (geoland2 project). The GEOV2 and GEOV1 products were produced by VITO through the Copernicus Global Land Service. We acknowledge NASA for the MODIS products, and CEOS WGCV LPV for providing DIRECT 2.0 ground data. This study contributes to the CSIC-PTI TELEDETECT.

Appendix A. Supplementary data

Supplementary data to this article can be found online at https://doi.org/10.1016/j.jag.2023.103479.

References

Baret, F., Hagolle, O., Geiger, B., Bicheron, P., Miras, B., Huc, M., Berthelot, B., Niño, F., Weiss, M., Samain, O., Roujean, J.L., Leroy, M., 2007. LAI, fAPAR and fCover CYCLOPES global products derived from VEGETATION. Part 1: Principles of the algorithm. Remote Sens. Environ. 110 (3), 275–286.

Baret, F., Weiss, M., Lacaze, R., Camacho, F., Makhmara, H., Pacholcyzk, P., Smets, B., 2013. GEOV1: LAI, FAPAR Essential Climate Variables and FCOVER global time series capitalizing over existing products. Part1: Principles of development and production. Remote Sens. Environ. 137, 299–309.

Bayat, B., Camacho, F., Nickeson, J., Cosh, M., Bolten, J., Vereecken, H., Montzka, C., 2021. Toward operational validation systems for global satellite-based terrestrial essential climate variables. Int. J. Appl. Earth Obs. Geoinf. 95, 102240.

Bórnez, K., Descals, A., Verger, A., Peñuelas, J., 2020. Land surface phenology from VEGETATION and PROBA-V data. Assessment over deciduous forests. Int. J. Appl. Earth Obs. Geoinf. 84, 101974.

Buchhorn, M., Smets, B., Bertels, L., Roo, B.D., Lesiv, M., Tsendbazar, N.-E., Herold, M., Fritz, S., 2020. Copernicus Global Land Service: Land Cover 100m: collection 3: epoch 2015: Globe. Zenodo.

Camacho, F., Cernicharo, J., Lacaze, R., Baret, F., Weiss, M., 2013. GEOV1: LAI, FAPAR Essential Climate Variables and FCOVER global time series capitalizing over existing products. Part 2: Validation and intercomparison with reference products. Remote Sens. Environ. 137, 310–329.

Cammalleri, C., Verger, A., Lacaze, R., Vogt, J.V., 2019. Harmonization of GEOV2 fAPAR time series through MODIS data for global drought monitoring. Int. J. Appl. Earth Obs. Geoinf. 80, 1–12.

Campos-Taberner, M., García-Haro, F.J., Busetto, L., Ranghetti, L., Martínez, B., Gilabert, M.A., Camps-Valls, G., Camacho, F., Boschetti, M., 2018. A Critical Comparison of Remote Sensing Leaf Area Index Estimates over Rice-Cultivated Areas: From Sentinel-2 and Landsat-7/8 to MODIS, GEOV1 and EUMETSAT Polar System. Remote Sens. 10, 763.

CGLS, 2015. Copernicus Global land Component Product and Service Detailed Technical requirements to Technical Annex to Contract Notice 2015/S 151-277962 of 7th August 2015, https://land.copernicus.eu/global/sites/cgls.vito.be/files/service/EN-sAppendix%201%20to%20Annex%201%20of%20FWC_TA%20Global%20Land%20requirements%20%28appendix2TA%29_mdd_MC-JFP-4lots_CB_mc.pdf.

Cihlar, J., 1996. Identification of contaminated pixels in AVHRR composite images for studies of land biosphere. Remote Sens. Environ. 56 (3), 149–163.

Du, D., Zheng, C., Jia, L., Chen, Q., Jiang, M., Hu, G., Lu, J., 2022. Estimation of Global Cropland Gross Primary Production from Satellite Observations by Integrating Water Availability Variable in Light-Use-Efficiency Model. Remote Sens. 14, 1722.

Fang, H., Jiang, C., Li, W., Wei, S., Baret, F., Chen, J.M., Garcia-Haro, J., Liang, S., Liu, R., Myneni, R.B., Pinty, B., Xiao, Z., Zhu, Z., 2013. Characterization and intercomparison of global moderate resolution leaf area index (LAI) products: Analysis of climatologies and theoretical uncertainties. J. Geophys. Res. Biogeosci. 118 (2), 529–548.

Fang, H., Baret, F., Plummer, S., Schaepman-Strub, G., 2019a. An Overview of Global Leaf Area Index (LAI): Methods, Products, Validation, and Applications. Rev. Geophys. 57 (3), 739–799.

Fang, H., Zhang, Y., Wei, S., Li, W., Ye, Y., Sun, T., Liu, W., 2019b. Validation of global moderate resolution leaf area index (LAI) products over croplands in northeastern China. Remote Sens. Environ. 233, 111377.

Fang, H., Li, S., Zhang, Y., Wei, S., Wang, Y., 2021a. New insights of global vegetation structural properties through an analysis of canopy clumping index, fractional vegetation cover, and leaf area index. Sci. of Remote Sens. 4, 100027.

Fang, H., Wang, Y., Zhang, Y., Li, S., 2021b. Long-Term Variation of Global GEOV2 and MODIS Leaf Area Index (LAI) and Their Uncertainties: An Insight into the Product Stabilities. J. Remote Sens. 2021, 9842830.

Fernandes, R., Plummer, S., Nightingale, J., Baret, F., Camacho, F., Fang, H., Garrigues, S., Gobron, N., Lang, M.L., R., LeBlanc, S., Meroni, M., Martinez, B., Nilson, T., Pinty, B., Pisek, J., Sonnentag, O., Verger, A., Welles, J., Weiss, M., Widlowski, J.L., 2014. Global Leaf Area Index Product Validation Good Practices. Version 2.0. , in: G. Schaepman-Strub, M.R., & J. Nickeson (Ed.), Best Practice for Satellite-Derived Land Product Validation: Land Product Validation Subgroup (WGCV/CEOS) pp. 1-76.

Fuster, B., Sánchez-Zapero, J., Camacho, F., García-Santos, V., Verger, A., Lacaze, R., Weiss, M., Baret, F., Smets, B., 2020. Quality Assessment of PROBA-V LAI, fAPAR and fCOVER Collection 300 m Products of Copernicus Global Land Service. Remote Sens. 12, 1017.

Gcos, 2022. The 2022 GCOS ECVs Requirements. World Meteorological Organization, Geneva, Switzerland, p. 244. GCOS 245),.

GCOS, 2011. Global Climate Observing System - Systematic Observation Requirements for Satellite-Based Products for Climate, Supplemental Details to the Satellite Based Component of the Implementation Plan for the Global Observing System for Climate in Support of the UNFCCC (2010 Update), https://www.wmo.int/pages/prog/gcos/Publications/gcos-154.pdf. World Meteorological Organization, Geneva, Switzerland, p. 138.

Gobron, N., 2011. Ocean and Land Colour Instrument (OLCI) FAPAR and Rectified Channels over Terrestrial Surfaces Algorithm Theoretical Basis Document. European Commission Joint Research Centre, Ispra, Italy.

Huang, A., Shen, R., Di, W., Han, H., 2021. A methodology to reconstruct LAI time series data based on generative adversarial network and improved Savitzky-Golay filter. Int. J. Appl. Earth Obs. Geoinf. 105, 102633.

Jin, H., Li, A., Bian, J., Nan, X., Zhao, W., Zhang, Z., Yin, G., 2017. Intercomparison and validation of MODIS and GLASS leaf area index (LAI) products over mountain areas: A case study in southwestern China. Int. J. Appl. Earth Obs. Geoinf. 55, 52–67.

Kandasamy, S., Baret, F., Verger, A., Neveux, P., Weiss, M., 2013. A comparison of methods for smoothing and gap filling time series of remote sensing observations: application to MODIS LAI products. Biogeosci. 10, 4055–4071.

Lee, L.X., Whitby, T.G., Munger, J.W., Stonebrook, S.J., Friedl, M.A., 2023. Remote sensing of seasonal variation of LAI and fAPAR in a deciduous broadleaf forest. Agric. For. Meteorol. 333, 109389.

Lyapustin, A., Wang, Y., Xiong, X., Meister, G., Platnick, S., Levy, R., Franz, B., Korkin, S., Hilker, T., Tucker, J., Hall, F., Sellers, P., Wu, A., Angal, A., 2014. Scientific impact of MODIS C5 calibration degradation and C6+ improvements. Atmos. Meas. Tech. 7, 4353–4365.

McCallum, I., Wagner, W., Schmullius, C., Shvidenko, A., Obersteiner, M., Fritz, S., Nilsson, S., 2010. Comparison of four global FAPAR datasets over Northern Eurasia for the year 2000. Remote Sens. Environ. 114 (5), 941–949.

Mota, B., Gobron, N., Morgan, O., Cappucci, F., Lanconelli, C., Robustelli, M., 2021. Cross-ECV consistency at global scale: LAI and FAPAR changes. Remote Sens. Environ. 263, 112561.

Myneni, R.B., Hoffman, S., Knyazikhin, Y., Privette, J.L., Glassy, J., Tian, Y., Wang, Y., Song, X., Zhang, Y., Smith, G.R., Lotsch, A., Friedl, M., Morisette, J.T., Votava, P., Nemani, R.R., Running, S.W., 2002. Global products of vegetation leaf area and absorbed PAR from year one of MODIS data. Remote Sens. Environ. 83, 214–231.

Pinty, B., Clerici, M., Andredakis, I., Kaminski, T., Taberner, M., Verstraete, M.M., Gobron, N., Plummer, S., Widlowski, J.-L., 2011. Exploiting the MODIS albedos with the Two-stream Inversion Package (JRC-TIP): 2. Fractions of transmitted and absorbed fluxes in the vegetation and soil layers. J. Geophys. Res. 116 (D9).

Pu, J., Yan, K., Gao, S.i., Zhang, Y., Park, T., Sun, X., Weiss, M., Knyazikhin, Y., Myneni, R.B., 2023. Improving the MODIS LAI compositing using prior time-series information. Remote Sens. Environ. 287, 113493.

Roujean, J.L., Leroy, M., Deschamps, P.Y., 1992. A bidirectional reflectance model of the Earth's surface for the correction of remote sensing data. J. Geophys. Res. 97, 20455–20468.

Song, B., Liu, L., Zhao, J., Chen, X., Zhang, H., Gao, Y., Zhang, X., 2021. Validation of Four Coarse-Resolution Leaf Area Index Products Over Croplands in China Using Field Measurements. IEEE J. Sel. Top. Appl. Earth Obs. Remote Sens. 14, 9372–9382.

Steinberg, D.C., Goetz, S.J., Hyer, E.J., 2006. Validation of MODIS FPAR products in boreal forests of Alaska. IEEE Trans. Geosci. Remote Sens. 44, 1818–1828.

Toté, C., Swinnen, E., Sterckx, S., Benhadj, I., Dierckx, W., Gómez-Chova, L., Ramon, D., Stelzer, K., Heuvel, L.V.d., Clarijs, D., Niro, F., 2021. The Reprocessed Proba-V Collection 2: Product Validation, 2021 IEEE IGARSS, pp. 8084-8086.

Verger, A., Baret, F., Weiss, M., 2008. Performances of neural networks for deriving LAI estimates from existing CYCLOPES and MODIS products. Remote Sens. Environ. 112 (6), 2789–2803.

Verger, A., Baret, F., Weiss, M., 2011. A multisensor fusion approach to improve LAI time series. Remote Sens. Environ. 115 (10), 2460–2470.

Verger, A., Baret, F., Weiss, M., Kandasamy, S., Vermote, E., 2013. The CACAO method for smoothing, gap filling and characterizing seasonal anomalies in satellite time series. IEEE Trans. Geosci. Remote Sens. 51 (4), 1963–1972.

Verger, A., Baret, F., Weiss, M., 2014. Near real time vegetation monitoring at global scale. IEEE J. Sel. Top. Appl. Earth Obs. Remote Sens. 7 (8), 3473–3481.

Verger, A., Baret, F., Weiss, M., Filella, I., Peñuelas, J., 2015. GEOCLIM: A global climatology of LAI, FAPAR, and FCOVER from VEGETATION observations for 1999–2010. Remote Sens. Environ. 166, 126–137.

Verger, A., Baret , F., Weiss, M., 2020. Algorithm Theoretical Basis Document - GEOV2/AVHRR: Leaf Area Index (LAI), Fraction of Absorbed Photosynthetically Active Radiation (FAPAR) and Fraction of green Vegetation Cover (FCOVER) from LTDR AVHRR (Issue I2.50), Report for THEIA-SP-44-0207-CREAF, https://www.theia-land.fr/wp-content/uploads/2022/03/THEIA-SP-44-0207-CREAF_I2.50.pdf, p. 51.

Verger, A., Kandasamy, S., Baret, F., 2016. Temporal techniques in remote sensing of global vegetation. Springer, United States.

Verrelst, J., Muñoz, J., Alonso, L., Delegido, J., Rivera, J.P., Camps-Valls, G., Moreno, J., 2012. Machine learning regression algorithms for biophysical parameter retrieval: Opportunities for Sentinel-2 and -3. Remote Sens. Environ. 118, 127–139.

Weiss, M., Baret, F., Verger, A., 2014. BELMANIP2: Enhancement of the CEOS-BELMANIP ensemble of sites used for the validation of land products from medium resolution sensors. In: Sobrino, J. (Ed.), RAQRS, Valencia. Spain.

Xu, B., Li, J., Park, T., Liu, Q., Zeng, Y., Yin, G., Yan, K., Chen, C., Zhao, J., Fan, W., Knyazikhin, Y., Myneni, R.B., 2020. Improving leaf area index retrieval over heterogeneous surface mixed with water. Remote Sens. Environ. 240, 111700.

Yan, K., Park, T., Yan, G., Chen, C., Yang, B., Liu, Z., Nemani, R., Knyazikhin, Y., Myneni, R., 2016. Evaluation of MODIS LAI/FPAR Product Collection 6. Part 1: Consistency and Improvements. Remote Sens. 8, 359.

Yan, K., Park, T., Chen, C., Xu, B., Song, W., Yang, B., Zeng, Y., Liu, Z., Yan, G., Knyazikhin, Y., Myneni, R.B., 2018. Generating Global Products of LAI and FPAR From SNPP-VIIRS Data: Theoretical Background and Implementation. IEEE Trans. Geosci. Remote Sens. 56 (4), 2119–2137.

Yang, W., Shabanov, N.V., Huang, D., Wang, W., Dickinson, R.E., Nemani, R.R., Knyazikhin, Y., Myneni, R.B., 2006. Analysis of leaf area index products from combination of MODIS Terra and Aqua data. Remote Sens. Environ. 104 (3), 297–312.

Yin, G., Qu, Y., Verger, A., Li, J., Jia, K., Xie, Q., Liu, G., 2022. Smartphone Digital Photography for Fractional Vegetation Cover Estimation. Photogramm. Eng. Remote Sens. 88 (5), 303–310.

Yin, L., Tao, F., Chen, Y.i., Liu, F., Hu, J., 2021. Improving terrestrial evapotranspiration estimation across China during 2000–2018 with machine learning methods. J. Hydrol. 600, 126538.

Yu, H., Yin, G., Liu, G., Ye, Y., Qu, Y., Xu, B., Verger, A., 2021. Validation of Sentinel-2, MODIS, CGLS, SAF, GLASS and C3S Leaf Area Index Products in Maize Crops. Remote Sens. 13, 4529.

Zhang, Z., Zhang, Y., Zhang, Y., Gobron, N., Frankenberg, C., Wang, S., Li, Z., 2020. The potential of satellite FPAR product for GPP estimation: An indirect evaluation using solar-induced chlorophyll fluorescence. Remote Sens. Environ. 240, 111686.